Preprints of the 23rd IFAC World Congress
Busan, Republic of Korea, August 23-28, 2026

Fully Actuated System Approach for Nonlinear Systems With Uncontrollable Unstable Linearization ⋆

Dake Gu * **Yindong Liu** *

* *School of Automation Engineering, Northeast Electric Power University, Jilin City, China (e-mail: gudake@neepu.edu.cn, y.d.liu@163.com).*

Abstract: This paper investigates a class of nonlinear chained systems with odd-power input channels and uncontrollable unstable linearization. Instead of pursuing global smooth stabilization, which is impossible for this class, a sub-fully actuated system formulation is developed by successively differentiating the output. This transformation makes the input gain and its singularity set explicit. Recursive reconstruction maps are then introduced to express the state variables in the output-jet space, allowing the singularity boundaries to be characterized in terms of the closed-loop linear dynamics. A real odd-root feedback law is designed to impose assignable linear input-output dynamics on the nonsingular feasible domain. To address singularity avoidance, a constructive zero-crossing test is provided to determine whether a given initial condition belongs to the region of exponential attraction before simulation. The behavior of the controller near singular boundaries is also discussed. Numerical examples illustrate both admissible trajectories and boundary-crossing cases, thereby clarifying the scope and limitation of the proposed substabilizing controller.

Keywords: Fully actuated system (FAS), regions of exponential attraction, nontriangular systems, singularity set, substabilization.

1. INTRODUCTION

Nonlinear systems in which the control input appears through odd-power channels and propagates along a lower-triangular state structure arise in several control contexts, yet they do not fall within the scope of conventional smooth stabilization techniques. Even when their vector fields are smooth, the loss of influence of the input on specific state components creates regions in which smooth feedback cannot enforce asymptotic convergence.

This benchmark system in 2-dimension (1) was originally analyzed by Aeyels (1985), who established the impossibility of smooth state-feedback stabilization.

$$\begin{cases} \dot{x}_1 = x_1 + x_2^3, \\ \dot{x}_2 = u, \end{cases} \tag{1}$$

Bacciotti (1991) later confirmed this fundamental limitation. The underlying reason, as clarified in Qian and Lin (2002), is that the system's linearization possesses an unstable, uncontrollable mode, thereby excluding any differentiable $(\mathbb{C}^r, r \geq 1)$ stabilizing control law.

Kawski (1989) provided a significant contribution by developing a locally Hölder-continuous stabilizer for this model. His controller took the structure

$$u = ax_2 + bx_1^{1/3},$$

guaranteeing asymptotic stability under the condition $b > a > 1$. A subsequent advance was made by Qian and Lin (2002), who synthesized a globally stabilizing continuous-yet non-smooth-feedback law, achieving strong stability in the Kurzweil sense.

The system is also cited in controllability studies Terrell (2009), where it is demonstrated to be globally controllable on the plane. A recent extension by Zou et al. (2020) introduced an uncertain variant with bounded unknown parameters. The proposed feedback gains in their work reduce, in the nominal case, to a form that induces oscillatory closed-loop behavior for the original benchmark problem.

Very recently, Duan (2022) revealed that this system is equivalent to a sub-FAS with the singularity set containing the origin. It can be treated with the fully actuated systems (FAS) approach Duan (2021a,b,c,d,e, 2023). Consequently, every trajectory originating within this defined domain converges to the origin at an exponential rate. The analysis further reveals that an exact characterization of this domain enables the attainment of global asymptotic stability. This can be accomplished in two ways: by integrating the designed controller with a pre-existing globally stabilizing law, or by employing a preliminary control stage that steers any initial state outside the domain into it.

It should be emphasized that the purpose of the present work is not to replace existing globally stabilizing nons-

⋆ This work was supported by the Department of Education of Jilin Province (Grant No. JJKH20250876KJ), the Department of Science and Technology of Jilin Province (Grant No. 20250205060GH) and the National Natural Science Foundation of China (Grant No. 62188101).

©2026 the authors. Accepted by IFAC for publication under a Creative Commons Licence CC-BY-NC-ND

mooth feedback laws. Those methods are powerful when global asymptotic stabilization is the only objective. The motivation here is different: by using the sub-FAS representation, one obtains assignable linear input-output dynamics, an explicit input-gain singularity structure, and a computable description of the nonsingular operating region. Therefore, the proposed method trades globality for transparent closed-loop pole assignment and explicit singularity geometry. This trade-off is useful when the controller is required to operate inside a prescribed nonsingular domain or when a preliminary controller can first steer the state into such a domain.

The main contributions are summarized as follows. First, a class of odd-power chained nonlinear systems is rewritten into a high-order sub-FAS model with an explicit polynomial input gain. Second, recursive output-jet reconstruction maps are derived, which make the singularity set visible in the jet space. Third, a odd-root feedback law is proposed to assign linear input-output dynamics on the nonsingular feasible domain. Fourth, a constructive zero-crossing condition is introduced to verify singularity avoidance a priori. Finally, the illustrative example is revised to show both admissible and inadmissible initial conditions, thereby demonstrating the boundary of the proposed substabilizing mechanism.

The remainder of this article is organised as follows. The problem formulation is presented in Section 2. In Section 3, the model construction, the reconstruction maps, the controller design and the substability analysis are proposed, respectively. Section **??** concludes with a numerical example illustrating the proposed method.

2. PROBLEM FORMULATION

Consider the feedback stabilization problem for a class of $n-$ dimensional nonlinear systems of the following form

$$\begin{aligned} \dot{x}_1 &= x_2^{p_1} + \phi_1(x_1) \\ \dot{x}_2 &= x_3^{p_2} + \phi_2(x_1, x_2) \\ &\vdots \\ \dot{x}_n &= u^{p_n} + \phi_n(x_1, \ldots, x_n) \end{aligned} \tag{2}$$

where $x = (x_1, \ldots, x_n)^{\mathrm{T}} \in \mathbb{R}^n$ and $u \in \mathbb{R}$ are the system state and input, respectively. For $i = 1, \ldots, n$, the function $\phi_i : \mathbb{R}^i \to \mathbb{R}^1$, is continuously differentiable and p_i is an odd positive integer.

Assumption 1. The functions $\phi_i, i = 1, 2, \ldots, n$ are sufficiently smooth for the successive output differentiations used below. Moreover, $\phi_i(0, \ldots, 0) = 0$, so that the origin is an equilibrium of the open-loop system under $u = 0$.

3. MAIN RESULTS

3.1 Recursive Differentiation and Model Construction

Let the system output be

$$y = x_1. \tag{3}$$

The objective of this section is to derive a differential equation of order n in which the control input u^{p_n} appear explicitly and linearly.

- First Derivative: The first derivative follows directly from (3):
$$\dot{y} = \dot{x}_1 = x_2^{p_1} + \phi_1(y). \tag{4}$$
This equation defines the first virtual control, x_2, in terms of y and $\dot{y}$.
- Second Derivative: Differentiating (4) and substituting the dynamics from (2), we have
$$\begin{aligned} \ddot{y} &= \frac{\mathrm{d}}{\mathrm{d}t}\left[x_2^{p_1} + \phi_1(y)\right] \\ &= p_1 x_2^{p_1-1}\dot{x}_2 + \frac{\partial \phi_1}{\partial y}\dot{y} \\ &= p_1 x_2^{p_1-1}\left(x_3^{p_2} + \phi_2(x_1, x_2)\right) + \frac{\partial \phi_1}{\partial y}\dot{y}. \end{aligned} \tag{5}$$
Equation (5) can be rewritten as:
$$\ddot{y} = F_2(x_2, y, \dot{y}) + G_2(x_2) \cdot x_3^{p_2}, \tag{6}$$
where $F_2(\cdot) = p_1 x_2^{p_1-1}\phi_2(x_1, x_2) + \frac{\partial \phi_1}{\partial y}\dot{y}$ and $G_2(\cdot) = p_1 x_2^{p_1-1}$ are smooth functions of the argument $(x_2, y, \dot{y})$, and x_3 appears as the new virtual control.
- General k-th Derivative: Proceeding by induction, assume that the $(k-1)$-th derivative of the output admits the form:
$$\begin{aligned} y^{(k-1)} = {} & F_{k-1}(x_2, \ldots, x_{k-1}, y, \ldots, y^{(k-2)}) \\ & + G_{k-1}(x_2, \ldots, x_{k-1}) \cdot x_k^{p_{k-1}}. \end{aligned} \tag{7}$$
Differentiating (7) and substituting $\dot{x}_k$ yields:
$$\begin{aligned} y^{(k)} &= \frac{\mathrm{d}F_{k-1}}{\mathrm{d}t} + \frac{\mathrm{d}G_{k-1}}{\mathrm{d}t}x_k^{p_{k-1}} + G_{k-1}p_{k-1}x_k^{p_{k-1}-1}\dot{x}_k \\ &= \underbrace{\frac{\mathrm{d}F_{k-1}}{\mathrm{d}t} + \frac{\mathrm{d}G_{k-1}}{\mathrm{d}t}x_k^{p_{k-1}} + G_{k-1}p_{k-1}x_k^{p_{k-1}-1}\phi_k}_{F_k(x_2, \ldots, x_k, y, \ldots, y^{(k-1)})} \\ &\quad + \underbrace{G_{k-1}p_{k-1}x_k^{p_{k-1}-1}}_{G_k(x_2, \ldots, x_k)} \cdot x_{k+1}^{p_k}. \end{aligned} \tag{8}$$
Thus, the recursive structure is derived. The functions F_k and G_k are smooth and depend only on $(x_2, \ldots, x_k, y, \ldots, y^{(k)})$ and $(x_2, \ldots, x_k)$, respectively.
- n-th Derivative and Sub-FAS Model: Applying the recursive step for $k = n$ culminates in the n-th order differential equation:
$$y^{(n)} = F_n(x, y, \ldots, y^{(n-1)}) + G_n(x) \cdot u^{p_n}, \tag{9}$$
with
$$G_n(x) = \left(\prod_{i=1}^{n-1} p_i\right)\left(\prod_{i=2}^{n} x_i^{p_{i-1}-1}\right). \tag{10}$$

Equation (9) is the sub-FAS model of (2). The above deduction shows that a class of nonlinear systems, non-feedback-linearizable, odd-power chained nonlinear systems admits explicit high-order sub-FAS representation, with a closed-form gain G_n that is polynomial in the virtual states.

3.2 Singular Set and Feasible Set

Since the control design will require division by $G_n(x)$, that is, where $G_n(x)$ vanishes must be excluded. We define the following singular set:

$$\mathcal{S} = \{x \in \mathbb{R}^n | G_n(x) = 0\} = \bigcup_{i=2, p_{i-1}>1}^{n} \{x_i = 0\}, \tag{11}$$

and the feasible set clearly has the following expression:

$$\mathcal{F} = \mathbb{R}^n \setminus \mathcal{S} = \{x \in \mathbb{R}^n | x_i \neq 0, i = 2, \ldots, n\}. \tag{12}$$

The feasible set $\mathcal{F}$ is not a conventional neighborhood of the origin, because the origin itself belongs to the singular set $\mathcal{S}$. Therefore, classical Lyapunov stability with respect to a full neighborhood of the origin cannot be expected. The role of $\mathcal{F}$ is to specify the nonsingular domain on which the sub-FAS inversion is meaningful. A trajectory may converge to the origin only asymptotically while approaching the singular set in the limit; hence the essential issue is not uniform separation from $\mathcal{S}$, but avoidance of finite-time crossing of the singular hypersurfaces.

3.3 State Reconstruction via Output and its Derivatives

To facilitate the analysis of substability and to characterize the singularity set within the jet space of the output, the state variables x_i must be reconstructed from the output y and its derivatives. Let

$$z = [y, \dot{y}, \ldots, y^{(n-1)}]^{\mathrm{T}} \in \mathbb{R}^n \tag{13}$$

denote the output-jet vector. On an appropriate feasible jet domain, there exist smooth map $\Psi_i : \mathbb{R}^n \to \mathbb{R}$ such that

$$x_i = \Psi_i(z), i = 1, \ldots, n. \tag{14}$$

Introduce the odd-root operator

$$\mathrm{root}_p(\cdot) := \mathrm{sgn}(\cdot)|\cdot|^{1/p}, \tag{15}$$

where p is an odd integer. The map $\mathrm{root}_p(r) = \mathrm{sgn}(r)|r|^{1/p}$ is continuous on $\mathbb{R}$ and smooth on $\mathbb{R} \setminus \{0\}$. It is generally not differentiable at $r = 0$ when $p > 1$. In the present reconstruction, smoothness is therefore claimed only on connected components of the jet domain where the corresponding residuals and intermediate gains do not vanish.

The first coordinate is immediate:

$$\Psi_1(z) = x_1 = y. \tag{16}$$

From (4),

$$\dot{y} = x_2^{p_1} + \phi_1(y) \Rightarrow x_2^{p_1} = \dot{y} - \phi_1(y).$$

Therefore

$$\begin{aligned} \Psi_2(z) = x_2 &= \mathrm{root}_{p_1}\left(\dot{y} - \phi_1(y)\right) \\ &= \mathrm{sgn}(\dot{y} - \phi_1(y))|\dot{y} - \phi_1(y)|^{1/p_1}. \end{aligned} \tag{17}$$

Using (6) and substituting $x_2 = \Psi_2(z)$, the second derivative of the output takes the following form

$$\ddot{y} = F_2(y, \dot{y}, \Psi_2(z)) + G_2\left(\Psi_2(z)\right) x_3^{p_2}.$$

Introduce the residual

$$R_3(z) := \ddot{y} - F_2(y, \dot{y}, \Psi_2(z)).$$

Then

$$R_3(z) = G_2\left(\Psi_2(z)\right) x_3^{p_2},$$

so that

$$x_3^{p_2} = \frac{R_3(z)}{G_2\left(\Psi_2(z)\right)}.$$

We therefore define

$$\begin{aligned} \Psi_3(z) &= \mathrm{root}_{p_2}\left(\frac{R_3(z)}{G_2\left(\Psi_2(z)\right)}\right) \\ &= \mathrm{sgn}\left(\frac{R_3(z)}{G_2\left(\Psi_2(z)\right)}\right)\left|\frac{R_3(z)}{G_2\left(\Psi_2(z)\right)}\right|^{1/p_2}. \end{aligned} \tag{18}$$

Furthermore, the higher components are obtained recursively by

$$\begin{aligned} \Psi_k(z) &= \mathrm{sgn}\left(\frac{R_k(z)}{G_{k-1}(\Psi_2(z), \ldots, \Psi_{k-1}(z))}\right) \\ &\quad \times \left|\frac{R_k(z)}{G_{k-1}(\Psi_2(z), \ldots, \Psi_{k-1}(z))}\right|^{1/p_{k-1}}, \\ &\quad k = 3, 4, \ldots, n, \end{aligned} \tag{19}$$

where R_k is the residual

$R_k(z) := y^{(k-1)} - F_{k-1}(y, \ldots, y^{(k-2)}, \Psi_2(z), \ldots, \Psi_{k-1}(z))$, and G_{k-1} is the intermediate gain from (14).

In summary, on any connected component of the feasible jet domain where the intermediate gains are nonzero and the reconstructed virtual states do not cross zero, the maps Ψ_i are smooth and provide a one-to-one correspondence between the state x and the output jet z.

3.4 Sub-FAS-Based Substabilizing Controller

With the sub-FAS representation (9) available, we provide the following theorem to solve substabilization problem.

Theorem 1. Let $\mathcal{F} \subset \mathbb{R}$ be the feasible set of sub-FAS (9), and $a_i > 0, i = 0, 1, \ldots, n-1$ be a set of arbitrarily given constants which makes the characteristic polynomial

$$D(s) = s^n + a_{n-1}s^{n-1} + \cdots + a_1 s + a_0 \tag{20}$$

be Hurwitz. Then, a real odd-root substabilizing feedback law for the sub-FAS (9) is given by

$$\begin{cases} u(x) = \mathrm{sgn}\left(\dfrac{v - F_n(x, y, \ldots, y^{(n-1)})}{G_n(x)}\right) \\ \qquad \times \left|\dfrac{v - F_n(x, y, \ldots, y^{(n-1)})}{G_n(x)}\right|^{1/p_n} \\ v = -\displaystyle\sum_{k=0}^{n-1} a_k y^{(k)}, x \in \mathcal{F}. \end{cases} \tag{21}$$

Furthermore, for any trajectory that remain in $\mathcal{F}$, the closed-loop dynamics satisfy

$$y^{(n)} + a_{n-1}y^{(n-1)} + \cdots + a_1\dot{y} + a_0 y = 0, \tag{22}$$

and thus converge exponentially to the origin.

Proof. Substituting (21) into the sub-FAS model (9) yields

$$\begin{aligned} y^{(n)} &= F_n(x, \cdot) + G_{(n)}(x)u^{p_n} \\ &= F_n(x, \cdot) + G_{(n)}(x)\frac{v - F_n(x, \cdot)}{G_n(x)} = v \\ &= -a_{n-1}y^{(n-1)} - a_{n-2}y^{(n-2)} - \cdots - a_0 y. \end{aligned}$$

Since (20) is Hurwitz, the closed-loop dynamics (22) is exponentially stable, which implies exponential convergence of y and its derivatives along any trajectory that remains in $\mathcal{F}$.

Remark 1. The feedback is well-defined for $x \in \mathcal{F}$. It is continuous wherever the argument of the odd-root is finite, and it is smooth on subsets where both $G_n(x) \neq 0$ and $v - F_n(x, \cdot) \neq 0$. Thus, the term smooth in this paper refers to smoothness on nonsingular components away from zero-crossings of the odd-root argument.

Remark 2. Theorem 1 extends the FAS compensation idea to a nonlinearly actuated, non-feedback-linearizable chain

system whose virtual channels are polynomial rather than linear. The feedback is globally smooth on $\mathcal{F}$ and produces exact linear closed-loop behavior, which, combined with Subsection 3.3, enables a precise substability and region of exponential attraction (ROEA) analysis.

Theorem 2. Let $A \in \mathbb{R}^{n\times n}$ be the companion matrix associated with the polynomial (20). Under the feedback law (21), the closed-loop output jet satisfies

$$\dot{z}(t) = Az(t), z(t) = e^{A(t-t_0)}z(t_0). \tag{23}$$

Define the Region of Exponential Attraction in jet space as

$$\mathcal{R} = \left\{ z_0 \in \mathbb{R}^n | \Psi_i(e^{A(t-t_0)}z_0) \neq 0, \forall t \geq t_0, i = 2, \ldots, n \right\}, \tag{24}$$

and in state space as

$$\mathcal{Q} = \{x_0 \in \mathbb{R}^n | x(t; x_0) \in \mathcal{F}, \forall t \geq 0\}. \tag{25}$$

Then,

(1) For all initial conditions $x_0 \in \mathcal{Q}$, the corresponding closed-loop trajectory converges exponentially to the origin;
(2) $\mathcal{Q}$ is an open subset of $\mathbb{R}^n$ and is in general nonconvex and unbounded;
(3) The origin belongs to the boundary of $\mathcal{Q}$, so the system is not Lyapunov stable in the classical neighborhood sense but is exponentially substabilized on $\mathcal{Q}$.

Proof. By Theorem 1, the output jet $z(t)$ evolves according to (23). By the deduction of susbection 3.3, $x_i = \Psi_i(z(t))$ on the feasible jet-domain, and the singular set corresponding to $\Psi_i(z(t)) = 0$ for $i \geq 2$. Thus the condition $z_0 \in \mathcal{R}$ is equivalent to $x(t; x_0) \notin \mathcal{S}$ for all $t \geq 0$, i.e. $x(t; x_0) \in \mathcal{F}$ for all the time, which characterizes $\mathcal{Q}$. Exponential convergence follow from (22) and (23).

Openness of Q is a consequence of continuous dependence of $z(t)$ and the Ψ_i on initial conditions together with the strict inequalities defining $\mathcal{R}$. Nonconvexity and unboundedness arise because the constraints $\Psi_i(e^{A(t-t_0)}z_0) \neq 0$ describe excluded tubes around singular trajectories in an otherwise unbounded linear system. The origin lies in $\mathcal{S}$ by Subsection 3.2 and is therefore on the boundary of $\mathcal{Q}$, which prevents classical Lyapunov stability but is consistent with substability.

Remark 3. Theorem 2 provides an explicit geometric characterization of the substable region of attraction for a non-feedback-linearizable chain system, expressed entirely in terms of the linear closed-loop matrix A and the reconstruction maps Ψ_i. This is significantly more informative than conventional local Lyapunov results: the region $\mathcal{Q}$ is not a small neighborhood but a potentially large, structured subset of the state space whose boundary is tied directly to the singular hyperplanes $\{x_i = 0\}$.

3.5 Constructive Singularity-Avoidance Test

Define the singularity functions in jet space.

$$\eta_2(z) = \dot{y} - \phi_1(y).$$

For $k \geq 3$, define

$$\eta_k(z) = R_k(z),$$

where $R_k(z)$ is the residual used in the reconstruction formula (19). Then $x_k = 0$ is equivalent to $\eta_k(z) = 0$, provided the previous reconstruction steps are nonsingular.

Under the feedback law, we have

$$z(t) = e^{A(t-t_0)}z_0.$$

Then, singularity avoidance can be checked by the proposition.

Proposition 1. Let z_0 be the output-jet vector corresponding to $x_0 \in \mathcal{F}$. Suppose that, for every $k = 2, \ldots, n$,

$$\eta_k(e^{A(t-t_0)}z_0) \neq 0, \forall t \geq t_0.$$

Then the closed-loop trajectory does not intersect the singular set in finite time. Consequently, the sub-FAS feedback remains well-defined for all finite t, and the output jet converges exponentially according to $z(t) = e^{A(t-t_0)}z_0$.

This condition is constructive because it does not require simulating the original nonlinear closed-loop system. For a given z_0, one only needs to test whether the explicitly known scalar functions $\eta_k(e^{A(t-t_0)}z_0)$ have zeros on $t \geq t_0$. In the illustrative example below, these functions reduce to exponential factors multiplied by quadratic polynomials, so the test becomes a direct root/discriminant check.

4. ILLUSTRATIVE EXAMPLE

4.1 Controller Design and Singularity Characterization

Consider the following three-dimensional system:

$$\begin{cases} \dot{x}_1 = x_2^3 + x_1, \\ \dot{x}_2 = x_3^3, \\ \dot{x}_3 = u^3. \end{cases} \tag{26}$$

This system is a special case of (2) with $p_1 = p_2 = p_3 = 3$, $\phi_1(x_1) = x_1$, and $\phi_2 = \phi_3 = 0$. Let

$$y = x_1.$$

Then

$$\dot{y} = x_2^3 + x_1, \tag{27}$$

and

$$\ddot{y} = 3x_2^2x_3^3 + x_2^3 + x_1. \tag{28}$$

Differentiating once more gives

$$y^{(3)} = 6x_2x_3^6 + 3x_2^2x_3^3 + x_2^3 + x_1 + 9x_2^2x_3^2u^3. \tag{29}$$

Therefore, the sub-FAS representation is

$$y^{(3)} = F_3(x) + G_3(x)u^3, \tag{30}$$

where

$$F_3(x) = 6x_2x_3^6 + 3x_2^2x_3^3 + x_2^3 + x_1,$$

and

$$G_3(x) = 9x_2^2x_3^2.$$

The singularity set is thus

$$\mathcal{S} = \{x_2 = 0\} \cup \{x_3 = 0\},$$

and the feasible set is

$$\mathcal{F} = \{x \in \mathbb{R}^3 \mid x_2 \neq 0,\ x_3 \neq 0\}.$$

Choose the desired characteristic polynomial as

$$D(s) = (s+1)^3 = s^3 + 3s^2 + 3s + 1.$$

The virtual input is selected as

$$v = -(y + 3\dot{y} + 3\ddot{y}).$$

Substituting (27) and (28) gives

$$v = -7x_1 - 6x_2^3 - 9x_2^2x_3^3.$$

Therefore,

$$v - F_3(x) = -8x_1 - 7x_2^3 - 12x_2^2x_3^3 - 6x_2x_3^6.$$

Solving (30) for u^3 yields

$$u^3 = \frac{-8x_1 - 7x_2^3 - 12x_2^2x_3^3 - 6x_2x_3^6}{9x_2^2x_3^2}.$$

Hence, the feedback law on $\mathcal{F}$ is

$$u(x) = \operatorname{sgn}\left(\frac{-8x_1 - 7x_2^3 - 12x_2^2x_3^3 - 6x_2x_3^6}{9x_2^2x_3^2}\right) \left|\frac{-8x_1 - 7x_2^3 - 12x_2^2x_3^3 - 6x_2x_3^6}{9x_2^2x_3^2}\right|^{1/3}. \quad (31)$$

Under this controller, the closed-loop input-output dynamics satisfy

$$y^{(3)} + 3\ddot{y} + 3\dot{y} + y = 0. \quad (32)$$

Next, we characterize the singularity condition in the output-jet space. From (27),

$$x_2 = \operatorname{root}_3(\dot{y} - y).$$

Moreover, from (28),

$$\ddot{y} - \dot{y} = 3x_2^2x_3^3.$$

Thus, when $x_2 \neq 0$,

$$x_3 = \operatorname{root}_3\left(\frac{\ddot{y} - \dot{y}}{3x_2^2}\right).$$

Therefore, the singularity hyperplanes in the output-jet space are

$$\dot{y} - y = 0, \qquad \ddot{y} - \dot{y} = 0. \quad (33)$$

Consequently, the ROEA associated with (31) can be written as

$$\mathcal{R}_{\text{ex}} = \left\{z_0 \in \mathbb{R}^3 \mid \dot{y}(t) - y(t) \neq 0,\ \ddot{y}(t) - \dot{y}(t) \neq 0,\ \forall t \geq 0\right\},$$

where $z(t) = [y(t), \dot{y}(t), \ddot{y}(t)]^{\mathrm{T}}$ is generated by (32). The corresponding state-space region is

$$\mathcal{Q}_{\text{ex}} = \{x_0 \in \mathcal{F} \mid x_2(t) \neq 0,\ x_3(t) \neq 0,\ \forall t \geq 0\}.$$

This characterization shows that belonging to the initial feasible set $\mathcal{F}$ is not sufficient. The initial condition must also ensure that the closed-loop output-jet trajectory avoids the singularity hyperplanes (33) for all finite time.

4.2 Simulation

This subsection verifies the closed-loop behavior of the proposed controller and illustrates the role of the ROEA condition. For the selected polynomial

$$D(s) = (s+1)^3,$$

the output response has the form

$$y(t) = e^{-t}(c_0 + c_1t + c_2t^2), \quad (34)$$

where

$$c_0 = y_0, \qquad c_1 = \dot{y}_0 + y_0, \qquad c_2 = \frac{\ddot{y}_0 + 2\dot{y}_0 + y_0}{2}. \quad (35)$$

Therefore, the singularity indicators can be checked directly before simulating the original nonlinear closed-loop system:

$$\dot{y}(t) - y(t) = e^{-t}\left[(c_1 - 2c_0) + (2c_2 - 2c_1)t - 2c_2t^2\right], \quad (36)$$

and

$$\ddot{y}(t) - \dot{y}(t) = e^{-t}\left[(2c_2 - 3c_1 + 2c_0) + (2c_1 - 6c_2)t + 2c_2t^2\right].$$

Case 1: First, consider the admissible initial condition

$$x(0) = [0.1, -0.6, 0.7]^{\mathrm{T}}. \quad (37)$$

From (27) and (28), the corresponding initial output jet is

$$z_0 = [0.1000, -0.1160, 0.2544]^{\mathrm{T}}.$$

Using (35), one obtains

$$y(t) = e^{-t}(0.1000 - 0.0160t + 0.06122t^2). \quad (38)$$

The two singularity indicators are

$$\dot{y}(t) - y(t) = e^{-t}(-0.2160 + 0.15444t - 0.12244t^2), \quad (39)$$

and

$$\ddot{y}(t) - \dot{y}(t) = e^{-t}(0.37044 - 0.39932t + 0.12244t^2). \quad (40)$$

The discriminants of the two quadratic polynomials in (39) and (40) are negative. Therefore, the first indicator is always negative and the second indicator is always positive for all $t \geq 0$. This proves a priori that the trajectory does not intersect the singular hyperplanes in finite time. Consequently, the feedback controller remains well-defined along the whole trajectory.

The simulation results for this admissible case are shown in Figs. 1-4. The states converge to the origin, while $x_2(t)$ and $x_3(t)$ do not cross zero during the transient process. The singularity indicators $\dot{y} - y$ and $\ddot{y} - \dot{y}$ keep fixed signs and approach zero only asymptotically. Meanwhile, $G_3(x(t)) = 9x_2^2(t)x_3^2(t)$ remains nonzero for every finite time. These results confirm that the trajectory stays inside the feasible domain $\mathcal{F}$ and converges exponentially to the origin.

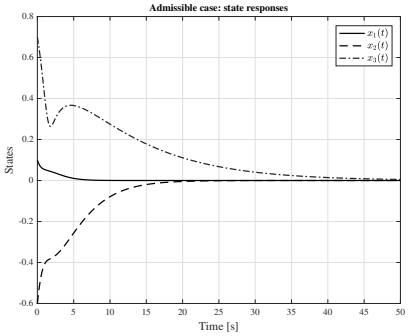


Fig. 1. State responses for the initial condition (37).

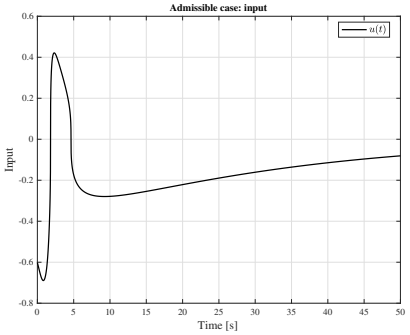


Fig. 2. Input for the initial condition (37).

Case 2: To further illustrate the necessity of the ROEA condition, consider the initial condition

$$x(0) = [0.5, 0.6, 0.7]^{\mathrm{T}}.$$

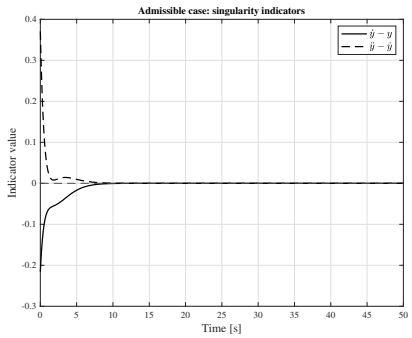


Fig. 3. Singularity indicators $\dot{y} - y$, $\ddot{y} - \dot{y}$ for the initial condition (37).

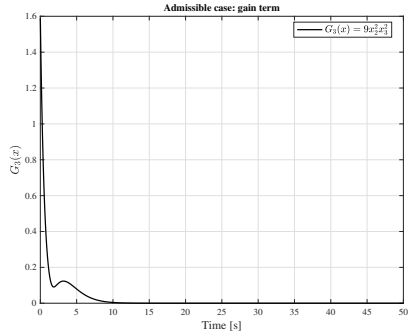


Fig. 4. Singularity indicator $G_3(x) = 9x_2^2x_3^2$ for the initial condition (37).

Although this point belongs to $\mathcal{F}$ at $t = 0$, it does not belong to the ROEA generated by the selected pole placement. In this case,

$$z_0 = [0.5000, 0.7160, 1.0864]^{\mathrm{T}},$$

and

$$y(t) = e^{-t}(0.5000 + 1.2160t + 1.50922t^2).$$

The second singularity indicator becomes

$$\ddot{y}(t) - \dot{y}(t) = e^{-t}(0.37044 - 6.62332t + 3.01844t^2),$$

which has a positive zero at approximately

$$t = 0.0574 \text{ s}.$$

Therefore, $x_3(t)$ reaches zero in finite time, and the sub-FAS inverse becomes invalid. Moreover,

$$\dot{y}(t) - y(t) = e^{-t}(0.2160 + 0.58644t - 3.01844t^2),$$

which also has a positive zero at approximately

$$t = 0.3817 \text{ s}.$$

This boundary-crossing case demonstrates that the feasible set $\mathcal{F}$ alone is not an invariant attraction region. The proposed controller achieves exponential substabilization only for initial conditions whose closed-loop output-jet trajectories avoid the singularity hyperplanes for all finite time.

The two cases above clarify the practical meaning of the ROEA characterization. The first case verifies exponential substabilization on an admissible trajectory, whereas the second case shows that the controller loses validity when the assigned linear jet dynamics drive the trajectory to the singular boundary. Therefore, in practical implementation, the proposed controller should be combined with the singularity-avoidance test or with a switching mechanism that prevents the state from approaching $G_3(x) = 0$.

5. CONCLUSION

This paper developed a sub-FAS-based substabilization method for a class of odd-power chained nonlinear systems with uncontrollable unstable linearization. The proposed transformation exposes the input-gain singularities and enables linear input-output pole assignment on nonsingular components of the feasible domain. A constructive jet-space zero-crossing test was introduced to verify whether a given initial condition avoids the singular set under the assigned closed-loop dynamics. The analysis also clarified that the controller is not a global smooth stabilizer; rather, it provides exponential substability on an explicitly characterized nonsingular region. Simulations with both admissible and boundary-crossing initial conditions confirmed the theoretical prediction and illustrated the practical role of singularity monitoring. Future work will consider robust switching mechanisms, uncertain dynamics, and multi-input extensions.

REFERENCES

Aeyels, D. (1985). Stabilization of a class of nonlinear systems by a smooth feedback control. *Systems & Control Letters*, 5(5), 289–294.

Bacciotti, A. (1991). *Local Stabilizability of Nonlinear Control Systems*. World Scientific.

Duan, G.R. (2023). Substability and substabilization: Control of subfully actuated systems. *IEEE Transactions on Cybernetics*, 53(11), 7309–7322.

Duan, G. (2021a). High-order fully actuated system approaches: Part I. models and basic procedure. *International Journal of Systems Science*, 52(2), 422–435.

Duan, G. (2021b). High-order fully actuated system approaches: Part II. generalized strict-feedback systems. *International Journal of Systems Science*, 52(3), 437–454.

Duan, G. (2021c). High-order fully actuated system approaches: Part III. robust control and high-order backstepping. *International Journal of Systems Science*, 52(5), 952–971.

Duan, G. (2021d). High-order fully actuated system approaches: Part IV. adaptive control and high-order backstepping. *International Journal of Systems Science*, 52(5), 972–989.

Duan, G. (2021e). High-order fully actuated system approaches: Part V. robust adaptive control. *International Journal of Systems Science*, 52(10), 2129–2143.

Duan, G. (2022). Stabilization via fully actuated system approach: A case study. *Journal of Systems Science and Complexity*, 35(3), 731–747.

Kawski, M. (1989). Stabilization of nonlinear systems in the plane. *Systems & Control Letters*, 12(2), 169–175.

Qian, C. and Lin, W. (2002). Practical output tracking of nonlinear systems with uncontrollable unstable linearization. *IEEE Transactions on Automatic Control*, 47(1), 21–36.

Terrell, W.J. (2009). *Stability and Stabilization: An Introduction*. Princeton University Press, Princeton.

Zou, Y., Qian, C., and He, S. (2020). A necessary and sufficient condition for stability of a class of planar nonlinear systems. *Automatica*, 121, 109198.